Journal of Biomolecular NMR, 9 (1997) 35–46
ESCOM

J-Bio NMR 407

Resonance assignment and secondary structure determination and stability of the recombinant human uteroglobin with heteronuclear multidimensional NMR

Teresa Carlomagno[a], Giuditta Mantile[b,*], Renzo Bazzo[c], Lucio Miele[b,**], Livio Paolillo[a], Anil B. Mukherjee[b] and Gaetano Barbato[c,***]

[a]*Department of Chemistry, University of Naples 'Federico II', Via Mezzocannone 4, I-80100 Naples, Italy*
[b]*Section on Developmental Genetics, Heritable Disorders Branch, Building 10, Room 9S241, NIH, Bethesda, MD 20892-1830, U.S.A.*
[c]*IRBM P. Angeletti, Spa., Via Pontina km 30.600, I-00040 Pomezia, Rome, Italy*

Received 7 December 1995
Accepted 8 October 1996

Keywords: Secondary structure; Uteroglobin; h-cc10kDa

Summary

Human uteroglobin (h-UG) or Clara cell 10kDa (cc10kDa) is a steroid-dependent, 17 kDa homodimeric, secretory protein with potent anti-inflammatory/immunomodulatory properties. However, the exact physiological role still remains to be determined. It has been hypothesised that its activity is exerted through the binding of a specific target represented by a small molecule (still unknown), and that the binding is regulated by the formation/disruption of two cysteine bonds. The binding properties of the reduced UG have been proved in vitro for several different molecules, but no in vivo data are available to date. However, binding has been observed between reduced rabbit UG and a protein of an apparent molecular mass of 90 kDa and, more recently, we found an h-UG-binding protein (putative receptor), of an apparent molecular mass of 190 kDa, on the surface of several cell types. The recognition involves oxidised h-UG. These findings pose the problem of the relevance of the oxidation state in the recognition process. To determine the solution structure of the oxidised h-UG, we produced wild-type as well as uniformly ^{15}N- and $^{15}N/^{13}C$-labelled samples of the recombinant protein. The assignments of the ^{1}H, ^{15}N and ^{13}C resonances are presented, based on a series of homonuclear 2D and 3D and heteronuclear 2D and 3D double and triple resonance NMR experiments. Our results indicate that h-UG is an extremely stable protein under a wide range of temperatures and pH conditions. The secondary structure in solution is in general agreement with previously reported crystal structures of rabbit UG, suggesting that cc10kDa and h-UG are indeed the same protein. Small local differences found in the N- and C-terminal helices seem to support the hypothesis that flexibility involves these residues; moreover, it possibly accounts for the residual binding properties observed when the protein is in the oxidised state.

Introduction

The mucosal epithelia of mammalian organs communicating to the external environment are chronically exposed to numerous antigens which can elicit inflammatory reactions either via activation of the immunological system or by a nonspecific physicochemical mechanism. To protect the integrity of the mucosal surface and to prevent constant activation of the immunological system by foreign antigens, it has been suggested that, during evolution, higher organisms may have adopted mechanisms to prevent undue damage caused by the inadvertent activation of inflammatory reactions (Mukherjee et al., 1988). One of these mechanisms, most extensively investigated in the

*Present address: Laboratory of Cardiovascular Science, Gerontology Research Center, NIA, Baltimore, MD 21224, U.S.A.
**Present address: FDA/CBER/DMA/LCB, Building 29, Room 225 HFM-558, Bethesda, MD 20892, U.S.A.
***To whom correspondence should be addressed.

Abbreviations: DPP, dipalmitoylphosphatidylcholine; ECM, extracellular matrix; PI, phosphatidylinositol; SDS, sodium dodecylsulphate; SW, sweep width; States-TPPI, hypercomplex quadrature detection method; TPPI, time proportional increment quadrature detection method; UG, uteroglobin.
Supplementary Material: One table, containing the assignment of the ^{1}H, ^{15}N, $^{13}C^{\alpha}$ and $^{13}C^{\beta}$ resonances, is available on request from the authors.

rabbit, involves uteroglobin (UG), a steroid-dependent, immunomodulatory/anti-inflammatory, cytokine-like protein, secreted by most epithelia of rodents (for a review see Miele et al., 1987) and humans (Miele et al., 1994). The protein is a homodimer. Each monomer, consisting of 70 amino acid residues, is covalently linked in an antiparallel orientation by two interchain disulphide bonds: Cys^{3}(A)–Cys^{69}(B) and Cys^{3}(B)–Cys^{69}(A), where A and B indicate the monomers. The rabbit protein was first discovered in the uterus during early pregnancy and was called blastokinin (Krishnan and Daniel, 1967) or uteroglobin (Beier, 1968). Although a human uteroglobin-like (h-cc10kDa) protein has been detected in various organs, including the uterus (Cowan et al., 1986; Kikukawa et al., 1988), the lung (Dhanireddy et al., 1988) and the prostate (Manyak et al., 1988), this protein was first purified from bronchial lavage by Singh et al. (1988a), who named it Clara cell 10kDa protein as at that time it was thought to be Clara-cell-specific. The calculated molecular weight of the cc10kDa protein is 17 kDa. Its name originated from the fact that its electrophoretic mobility was consistent with the apparent molecular mass of a 10 kDa protein in non-denaturing SDS-PAGE (Singh et al., 1988a). Moreover, this protein has also been called progesterone-binding protein (Beato, 1977), polychlorinated biphenyl-binding protein (Nordlund-Moller et al., 1990), retinoic acid and retinol-binding protein (Lopez de Haro et al., 1994) (in the following we will always refer to it as uteroglobin (UG), explicitly referring to its species of origin). The in vitro binding properties of the uteroglobin family have been studied with different ligands. Rabbit UG binds to progesterone both under reduced and oxidised conditions, with an apparent affinity constant that diminishes by one order of magnitude in the latter case (Beato et al., 1977). A similar result has also been observed for the binding of retinoic acid and retinol to rabbit UG (Lopez de Haro et al., 1994). The binding of methylsulphonyl polychloro-biphenyls, a xenobiotic compound, to rat UG has also been studied under reduced and oxidised conditions (Gillner et al., 1988), and an apparent affinity constant of nanomolar order has been found for the former conditions while the authors do not mention its value in the latter conditions. However, they state that an increase in affinity is observed under reducing conditions, and explicitly show the data for an increase in the specific binding by a factor of 3 under reduced versus oxidised conditions. Altogether, these data indicate that the affinity of the protein for ligands is enhanced under reduced conditions, but there is still appreciable binding under oxidised conditions. Surprisingly, unlike rabbit UG, mouse and human UG do not appear to bind to progesterone (Singh et al., 1990). Unfortunately, no comparative studies have been performed to date for the other ligands described. In any case, the binding properties for this family of proteins are yet to be assessed: the natural ligand (if there is one) is still to be found.

Recently, Guy et al. (1992) have reported that surfactant-producing pulmonary alveolar type II cells synthesise and secrete UG, and have suggested that by inhibiting PLA_2 in the lung this protein may play a surfactant-protective role. However, the exact physiological role of UG has not yet been determined.

The cDNAs encoding human (Singh et al., 1988b), rat (Singh et al., 1990) and mouse (Ray et al., 1993; Singh et al., 1993) UG have been cloned and characterised. There is 56% sequence identity between mature rabbit UG and h-UG and 53% sequence identity between h-UG and rat UG. Both rabbit (Miele et al., 1990) and human (Mantile et al., 1993) recombinant uteroglobins have been expressed in *E. coli* and their biological properties have been determined. It has been shown (Miele et al., 1990; Mantile et al., 1993) that under non-denaturing conditions both recombinant proteins are 100% dimer. In fact, the recombinant rabbit and human UGs are dimerised within the bacteria. Functionally, both rabbit and human uteroglobins are virtually identical as they inhibit both group I and group II phospholipase A_2 (PLA_2: EC 3.1.1.4) activities (Levin et al., 1986; Miele et al., 1988; Camussi et al., 1990a,b; Di Rosa and Ialenti, 1990; Ialenti et al., 1990; Chan et al., 1991; Facchiano et al., 1991; Perretti et al., 1991; Tetta et al., 1991; Cabre et al., 1992; Lloret and Moreno, 1992) and are excellent transglutaminase (TG: EC 2.3.2.13) substrates (Miele et al., 1990; Mantile et al., 1993).

During the past few years, two different crystal structures of purified rabbit UG have been reported, with crystal space group $C222_1$ by Morize et al. (1987) and space group $P2_1$ by Bally and Delettre' (1989). A crystal structure of native UG purified from rat lung has been reported by Umland et al. (1992) (space group $P6_522$). The UG protein structures described by these investigators, available in the Brookhaven database, are very similar. They show that the two monomers are related by a pseudobinary axis and that each monomer is folded into four helices. An oblong hydrophobic pocket is observed inside the dimer; its boundaries are delimited mainly by helices 1, 3 and 4, while helix 2 plays a minor role in the definition of the cavity. Access to this cavity is closed by the two disulphide bonds, which should completely prevent access to the cavity in the oxidised state. The relevance of this cavity in functional terms has primarily been speculative. Recently, a crystal structure (*P*222 space group) of h-UG, purified from cadaveric lung, has been reported by Umland et al. (1994). These authors focused mainly on the fact that either dipalmitoylphosphatidylcholine (DPP) or phosphatidylinositol (PI) is bound to the protein. This may indicate that h-UG and possibly other proteins of this family may be found in surfactant in phospholipid-bound form. However, protein degradation in cadaveric lung and artifactual contamination of h-UG protein during extraction, as described by Umland et al. (1994), cannot be ruled out. Moreover, previous

studies with recombinant h-UG failed to show any binding of purified recombinant rabbit UG or h-UG to bacterial cell membrane phospholipids (Mantile et al., 1993). Recently, Diaz Gonzalez and Nieto (1995) found a UG-binding protein with a molecular mass of 90 kDa as determined by gel filtration. The binding has been shown to take place with reduced rabbit UG, microsomes and plasmatic membranes from rat liver. Moreover, we have found a high-affinity (36 nM) h-UG-binding protein on the cell membrane of several cell types (Kundu et al., 1996). The apparent molecular weight of this protein is 190 kDa, and the binding is with oxidised h-UG. Cells lacking this protein do not bind to h-UG. This indicates that recombinant h-UG does not interact with phospholipids of intact cell membranes. It is still to be established, by cloning the cDNAs, if these two UG-binding proteins are related to each other. These findings represent the first experimental evidence of an interaction taking place between UG and a putative cellular receptor, and it is not involving the binding of UG with a small target molecule.

The oxidation state of UG could have some relevance for the binding with these proteins. This prompted us to begin the structural study of h-UG in its oxidised state in solution. In this paper we present our structural data of recombinant h-UG protein overexpressed in *E. coli*. We found that the protein has an exceptional stability to temperature denaturation over a wide range of pH. Our structural data are essentially in agreement with the previously reported crystal structures, although small differences in the lengths of the first and last helices have been observed that could well account for the binding properties described under oxidised conditions. We found that each subunit is folded into four helices, and from the number of observed signals we infer that a symmetry axis must exist. However, a local asymmetry is expected since the NMR peaks often exhibit a distorted line shape or even a double character.

Materials and Methods

Protein expression and purification

Human UG protein was expressed in *E. coli* using a new expression system, suitably designed for proteins presenting disulphide bonds, as described previously (Miele et al., 1990). Wild-type, ^{15}N-labelled (>90% isotopic purity) and ^{15}N/^{13}C-labelled (>90% isotopic purity) proteins were obtained with this procedure. The correct formation of homodimers in each sample of the recombinant protein was tested with SDS-PAGE gel electrophoresis as described for rabbit UG (Miele et al., 1990).

CD spectroscopy

The recombinant wild-type protein was extensively dialysed with a 5.0 mM KCl solution at pH 6.0 and freeze-dried. The solutions used for CD measurements were prepared by proper dilution of a concentrated stock. Concentrations were checked by quantitative amino acid analysis. Solutions of 9.6 μM h-UG and 1.0 mM KCl were used for the single CD spectra. The final pH values (adjusted using 0.1 M HCl and 0.1 M KOH) were 3.5 and 6.2. The solutions for the thermal denaturation experiments had the same concentration of h-UG and 10 mM of phosphate buffer at either pH 3.5 or 6.2. CD measurements were carried out on a JASCO J710 spectrometer. The instrument was calibrated with a 0.1% aqueous solution of d_{10} camphor sulphonic acid. Water-jacketed cells of 0.1 cm path length were used in all the experiments. The temperature control was obtained with a circulating bath of 45% water and 55% diethylene glycol with a thermosensor inserted in the cell jacket. An extra plotter was connected to the output exit of the thermocouple to follow the linearity of the temperature increase. Thermal denaturation curves were acquired at a 4 °C/h speed gradient starting at 20 °C.

NMR spectroscopy

Samples for NMR measurements typically comprised 0.8–1.2 mM protein dimer in 95% H_2O / 5% D_2O, or in D_2O, containing 0.1 M KCl and 0.5 mM NaN_3 at pH 5.9 (for pD the direct meter reading is used). The optimal temperature was established by estimating ^{1}H T_2 values in the range of 25–50 °C by the acquisition of 1D jump-and-return experiments following the method suggested by Anglister et al. (1993). The NMR experiments were acquired at 45 °C for improved line widths; however, some experiments were recorded at 37 °C to resolve some assignment ambiguities. All the NMR experiments were carried out on a Bruker AMX500 spectrometer. Three different samples were used: wild-type, ^{15}N-labelled and ^{15}N/^{13}C doubly labelled.

The multidimensional experiments were generally acquired with a strategy that maximises the digital resolution (Kay et al., 1989b); the incremented delay was set equal to half the dwell time to obtain a 90°, –180° phase correction (Bax et al., 1991; Archer et al., 1992).

Experiments on the wild-type sample Homonuclear 2D COSY (Aue et al., 1976), HOHAHA (24 and 42 ms mixing times using an MLEV-17 pulse train) (Braunschweiler and Ernst, 1983; Bax and Davis, 1985) and NOESY (100 ms mixing time) (Jeener et al., 1979) spectra were recorded at 37 °C on an H_2O sample solution: SW 6024 Hz (t_1,t_2), ^{1}H carrier on the water resonance, TPPI (t_1), matrix size 200–256 (t_1) × 1K (t_2), water presaturation. 2D NOESY (100 and 200 ms) and HOHAHA (73 ms) experiments were also acquired on a sample dissolved in D_2O and at 37 °C: SW 4016 Hz (t_1,t_2), ^{1}H carrier 3.30 ppm, TPPI (t_1), matrix size 128 (t_1) × 1K (t_2). A homonuclear 3D HOHAHA-NOESY spectrum (Oschkinat et al., 1988; Griesinger et al., 1989) (HOHAHA mixing time: 40 ms; NOESY mixing time: 100 ms) was acquired with the

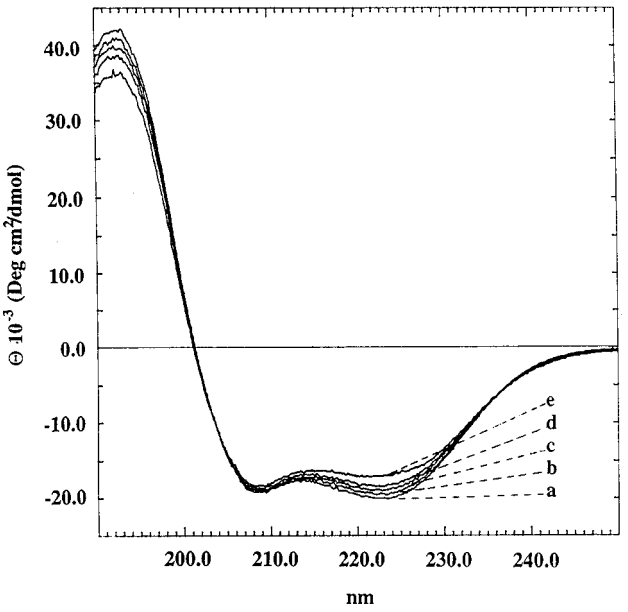

Fig. 1. Circular dichroism spectra at (a) 20 °C, (b) 30 °C, (c) 40 °C, (d) 50 °C and (e) 60 °C. The mean molar ellipticity (deg cm^2/dmol) is reported versus the wavelength (nm). The concentration of the protein used was about 9.6 μM (expressed in monomer units) and the pH was 6.2.

sample dissolved in H_2O: SW 6024 Hz (t_1,t_2,t_3), ^1H carrier on the water resonance, TPPI (t_1,t_2), matrix size 96 (t_1) × 64 (t_2) × 384 (t_3).

Experiments on the ^{15}N sample Unless otherwise stated, all the experiments were acquired on a sample dissolved in H_2O and at 45 °C. 2D ^{15}N-^1H HMQC correlation experiments with jump-return pulses for water suppression (Müller, 1979; Bax et al., 1983) and 2D HSQC spectra (Bodenhausen and Ruben, 1980; Bax et al., 1990a) with a 2 ms spin-lock for water suppression (Messerle et al., 1989) were acquired. The spectra were acquired with SW ^{15}N 1200 Hz, ^1H 6024 Hz, ^{15}N carrier 120.0 ppm, ^1H carrier on the water frequency, TPPI (t_1), matrix size 256 × 1024 and GARP heteronuclear decoupling. A 2D ^{15}N HSQC-HOHAHA (74 ms mixing time) (Gronenborn et al., 1989) experiment was acquired with the same settings of spectral width and carrier as described for the HSQC experiment and presaturation during the relaxation delay to suppress the water signal, TPPI (t_1) and matrix size 128 (t_1) × 2048 (t_2).

For the qualitative evaluation of the NH–solvent exchange rates, a series of 'fast' HMQC spectra (Marion et al., 1989a), matrix size 64 × 512, was collected at various times (12, 27, 42 and 136 min) on a freshly prepared sample of protein dissolved in D_2O. 3D heteronuclear HOHAHA-HMQC (mixing times 50 and 70 ms) (Marion et al., 1989b) and NOESY-HMQC (mixing times 100 and 200 ms) experiments (Kay et al., 1989a; Zuiderweg and Fesik, 1989) were acquired: SW 6000 (t_1), 1200 (t_2) and 2000 Hz (t_3), ^1H carrier 8.12 ppm, ^{15}N carrier 120.0 ppm, TPPI (t_1 with a phase shift of π/4, t_2), matrix size 32 (t_1) × 128 (t_2) × 512 (t_3), off-resonance DANTE water suppression.

Experiments on the $^{15}N/^{13}C$ sample Unless otherwise stated, all the experiments were acquired with the sample dissolved in D_2O and at 45 °C. A ^{13}C-^1H HSQC spectrum was acquired: SW 10 000 (t_1) and 6000 Hz (t_2), ^1H carrier 3.8 ppm, ^{13}C carrier 38.0 ppm, TPPI (t_1), matrix size 256 (t_1) × 1024 (t_2), GARP ^{13}C decoupling.

In order to assign $^{13}C^{\alpha}$ and $^{13}C^{\beta}$, an H(C)CH-COSY (Bax et al., 1990b; Ikura et al., 1991) and an (H)CCH-COSY with the t_1 semi-constant time method (Grzesiek and Bax, 1993) were acquired. H(C)CH-COSY spectrum: SW 3250 (t_1), 3750 (t_2) and 7500 Hz (t_3), ^1H carrier 3.0 ppm, ^{13}C carrier 45.0 ppm, States-TPPI (t_1,t_2), matrix size 80 (t_1) × 48 (t_2) × 512 (t_3), GARP ^{13}C decoupling. (H)CCH-COSY spectrum: SW 3750 (t_1), 8250 (t_2) and 7500 Hz (t_3), ^1H carrier 3.0 ppm, ^{13}C carrier 45.0 ppm, States-TPPI (t_1,t_2), matrix size 48 (t_1) × 96 (t_2) × 512 (t_3), GARP ^{13}C decoupling. Extensive folding of the carbon resonances was used in F2 for the H(C)CH-COSY and in F1 for the (H)CCH-COSY in order to reduce the spectral width (Bax et al., 1991).

A 3D ^{15}N-^{15}N-edited NOESY-HMQC (mixing time 150 ms) (Ikura et al., 1990) was performed on the doubly labelled sample dissolved in H_2O; SW 1200 (t_1 and t_2) and 3000 Hz (t_3), ^1H carrier 8.12 ppm and ^{15}N carrier 120.0 ppm, TPPI (t_1,t_2), matrix size 28 (t_1) × 28 (t_2) × 512 (t_3), off-resonance DANTE water suppression. A pulsed field gradient (PFG) 3D ^{15}N NOESY-HSQC experiment was performed on the doubly labelled sample dissolved in H_2O

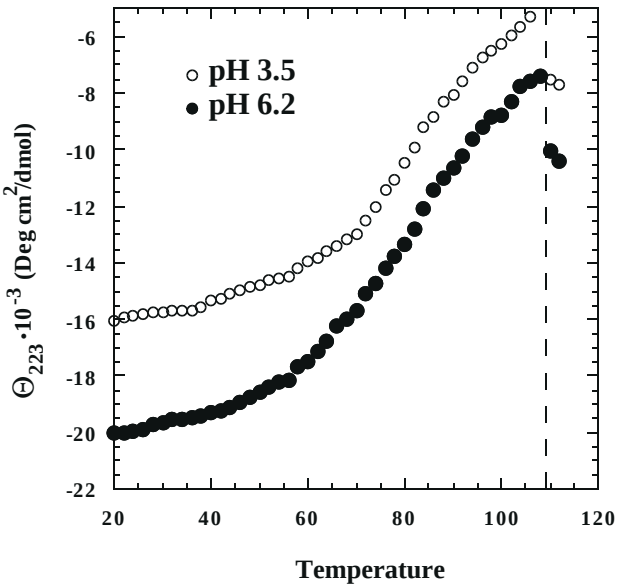

Fig. 2. Thermal denaturation curves at pH 6.2 (filled circles) and pH 3.5 (open circles). The mean molar ellipticity is reported at 223 nm. The linearity of the temperature increase was warranted up to 108 °C. For temperatures higher than 108 °C, i.e. points on the right side of the dashed line, the linearity is not assured; thus, these points are meaningless.

using z-field gradients (Sklenář et al., 1993). The ^{1}H carrier was in the middle of the ^{1}H spectrum during the first part of the NOESY step and shifted to the middle of the HN region during the NOESY mixing time to achieve better resolution in the acquisition dimension. Water suppression was achieved by the gradient-tailored excitation WATERGATE applied to protons for the acquisition step. Moreover, water suppression was improved by the use of gradients during the NOESY mixing time and during the first HSQC transfer step. For the selective pulse on the HN we used a hard pulse sequence of the type 3α-τ-9α-τ-19α-τ-19ατ-9α-τ-3α (26α=180°) where the phase of the component pulses was {0°,180°,0°,0°,180°, 0°}. This pulse train has been optimised by Sklenář et al. (1993) for off-resonance water suppression at offsets $\Delta\nu = \pm(2K+1)/2\tau$. The delay τ was 301.0 μs for an HN–water offset of 1660 Hz. The other acquisition parameters were similar to those used for the previously acquired ^{15}N NOESY-HMQC spectra. Decoupling of the ^{13}C resonances was achieved by means of 180° refocusing hard pulses during both t_1 and t_2. The carrier of the ^{13}C (t_1) frequency was at 35 ppm in order to decouple the carbon aliphatic region, and at 110 ppm so as to decouple the ^{15}N both from the carbonyls and the C^{α} during acquisition.

Data processing

All 2D and 3D NMR spectra were processed by using the Bruker UXNMR software on an X32 computer. In all the 3D ^{15}N heteronuclear experiments, the final absorptive matrix was 64 (t_1) × 256 (t_2) × 512 (t_3) points, except for the ^{15}N-^{15}N HMQC-NOESY-HMQC experiment whose final matrix was 128 (t_1) × 128 (t_2) × 1K (t_3) data points. In the ^{13}C heteronuclear experiments, the final matrices were 256 (^{1}H) × 128 (^{13}C) × 1K points (^{1}H acquisition). The weighting function applied in the F1 and F2 dimensions was a 60° shifted sine-bell window function, while a Gaussian-to-Lorentzian multiplication function was used in F3. ^{1}H chemical shifts are reported in ppm relative to TSP. ^{13}C and ^{15}N chemical shifts are referenced to TSP by the method of the fraction (Wishart et al., 1995).

Results

CD spectroscopy

In order to gather information about thermal stability and structure content as a function of pH, circular dichroism spectra of UG were obtained at two different pH conditions for temperatures ranging from 20 to 60 °C. The circular dichroism spectra at pH 6.2, for different temperatures, are shown in Fig. 1. The thermal denaturation of h-UG was attempted at pH values of 3.5 and 6.2. In Fig. 2 the mean molar ellipticity Θ is reported as a function of temperature at pH 3.5 and pH 6.2. From Fig. 1, it is evident that at pH 6.2 the helix content decreases as the temperature rises; this trend is also observed at pH 3.5 but the helicity content is considerably lower, about 20% (data not shown). However, for both pH values the decrease is only slightly appreciable in the range 20–50 °C and begins to be appreciable over 60 °C. The temperature denaturation failed to reach the plateau due to the impossibility of obtaining a linear gradient up to temperatures higher than 108 °C (Fig. 2) with our thermostated system. However, these measurements allowed us to establish a reasonable temperature range in which to perform optimised NMR experiments. From Fig. 2, it is evident that the decrease in molar ellipticity in the range 30–50 °C was sufficiently low (about 1.5×10^{-3} deg cm^2/dmol) to allow NMR experiments to be run in this temperature range.

NMR spectroscopy

From the monitoring of ^{1}H T_2 values in the temperature range of 25–50 °C by 1D jump-and-return experiments, considering the total envelope of the amide signals (Anglister et al., 1993), we obtain the following estimations: T = 300 K: $T_2 \sim 16$ ms; T = 310 K: $T_2 \sim 19$ ms; T = 318 K: $T_2 \sim 23$ ms. This result, together with the stability indications from CD spectroscopy, prompted us to use a temperature of 45 °C for further NMR experiments.

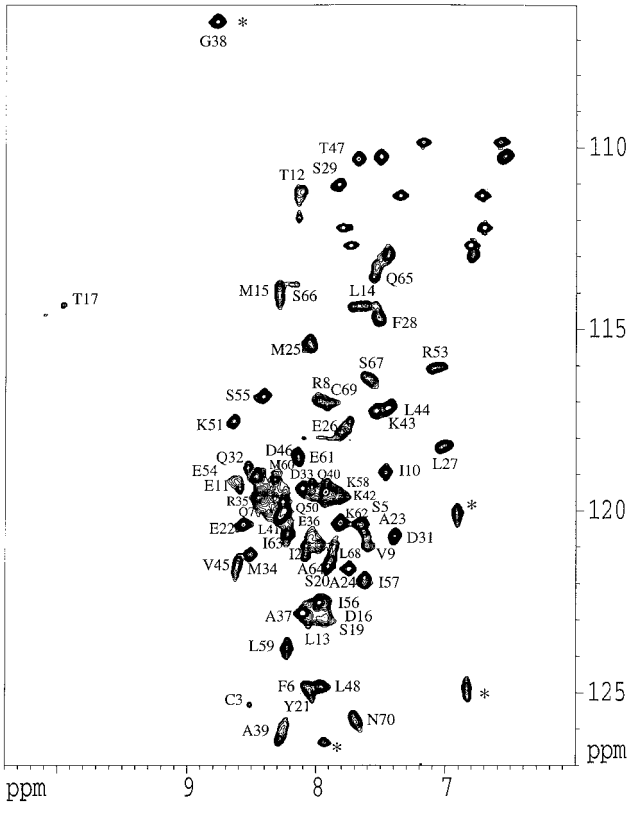

Fig. 3. Complete ^{1}H-^{15}N HSQC experiment, showing the assignments of all the amide signals. The residues Arg^8, Leu^{14}, Met^{15}, Met^{23}, Glu^{26}, Leu^{27}, Phe^{28}, Val^{45}, Met^{60}, Ala^{64}, Gln^{65} and Asn^{70} exhibit signals where the broadening and/or splitting by conformational exchange and/or asymmetry of the dimer is well evidenced. The asterisks indicate folded peaks.

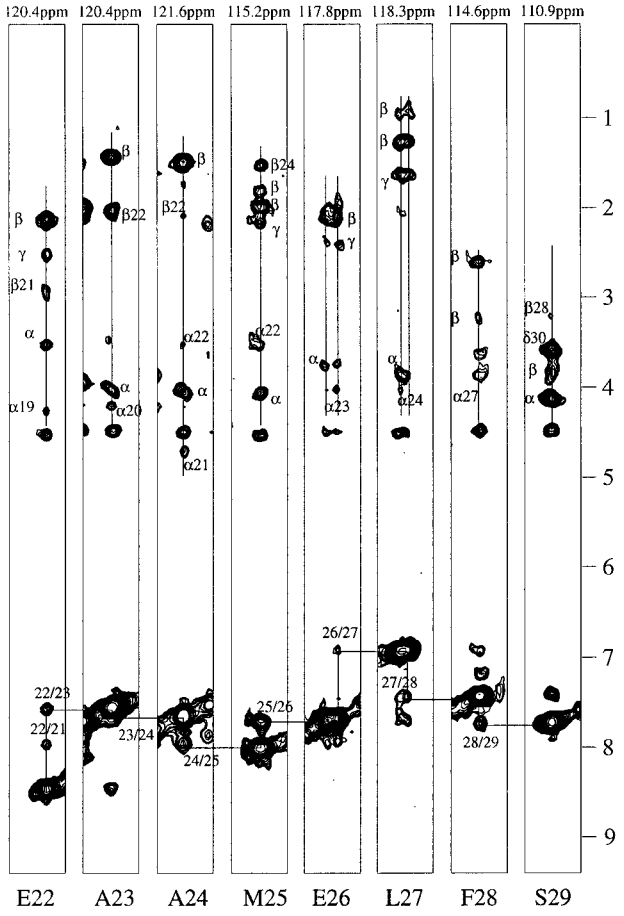

Fig. 4. Strip plot of the ^{15}N-edited 3D NOESY-HMQC experiment taken from planes at different ^{15}N chemical shifts (indicated at the top). The complete assignment of each signal and the HN-HN contacts for the residues Glu^{22}–Ser^{29} are evidenced with a solid line. Note the clear split of the signals of Glu^{26} and Leu^{27}, evidence of the existence of local asymmetry in the dimer. The asymmetry is likely responsible for the slightly different solvent exchange properties of the residues, depending on which monomer they belong to.

The homonuclear 2D NOESY and 2D HOHAHA spectra and the 3D HOHAHA-NOESY exhibited only few resolved cross peaks; however, they were very useful during the assignment process, as is mentioned later.

The ^{15}N HSQC spectrum is shown in Fig. 3. Almost all the signals are well resolved and were assigned. A total of 86 neat peaks can be identified (excluding the signals originating from side chains). Since the number of peaks observed is larger than the expected 64 (i.e. a total of 70 residues minus five prolines and the N-terminal residue) and some show a clear splitting into two very close but distinct peaks, we hypothesise a slight asymmetry in the dimer structure. Supporting experimental evidence also comes from the 3D ^{15}N heteronuclear spectra (both NOESY, Fig. 4, see residues 26 and 27, and HOHAHA, data not shown), where almost all the residues show two sets of resonances differing slightly for the amide resonance. A conformational equilibrium is taking place and has been evidenced by the 2D ^{15}N HSQC-HOHAHA spectrum, where we observed some exchange peaks between the amide resonances (data not shown). The intensity ratio of the two forms in equilibrium, as evaluated from ^{15}N HSQC, is not the same for all the residues, but ranges from 1:1 to 1:4. This difference is due to the effect of the water suppression system used, since in the spectra where gradients are used the ratio tends to be 1:1. This observation suggests the existence of different HN exchange rates for the two monomers, and this property is currently being investigated.

Identification of spin systems

The assignment of the ^{1}H, ^{15}N, $^{13}C^{\alpha}$ and $^{13}C^{\beta}$ resonances is shown in the Supplementary Material. Almost all the spin systems were identified by means of the 3D ^{15}N HOHAHA-HMQC spectra. A total of 58 different spin systems were observed from a total of 64 expected ones. The incomplete spin systems and the six lacking signals were identified by using the 2D 40 ms HOHAHA spectrum in H_2O and the 2D 73 ms HOHAHA spectrum in D_2O, and were confirmed with the HCCH-COSY-type experiments and 3D NOESY-HMQC and its PFG version. As a working method, we tried to confirm the assignment of all the residues with the HCCH-COSY spectra. In Fig. 5 the complete spin system pattern is reported for Thr^{17}, from both the HCCH-COSY-type experiments.

Sequential assignment

The sequence-specific assignment was achieved mainly by means of the $d_{NN}(i,i+1)$, $d_{\alpha N}(i,i+1)$ and $d_{\beta N}(i,i+1)$ connectivities in the 3D NOESY-HMQC spectrum and its PFG version of the ^{15}N- and ^{15}N/^{13}C-labelled UG following the guidelines indicated by Wüthrich (1986). In Fig. 6 the sequential NOE contacts as well as the NOEs that are informative for the secondary structure are reported.

A large sequential stretch of $d_{NN}(i,i+1)$, $d_{\alpha N}(i,i+1)$ and $d_{\beta N}(i,i+1)$ connectivities was observed from residues 19 to 52 (Fig. 6). The starting points were provided by the dipeptides Phe^{28}-Ser^{29} and Asp^{46}-Thr^{47}, and the tripeptide Ala^{37}-Gly^{38}-Ala^{39}. From these positions, moving in the direction of the N-terminus the assignment proceeded until position 19, while moving in the direction of the C-terminus the assignment reached position 52. The sequential assignment in the strand 19–52 was confirmed by the almost continuous presence of the connectivities $d_{\beta N}(i,i+1)$.

The series of $d_{NN}(i,i+1)$, $d_{\alpha N}(i,i+1)$ and $d_{\beta N}(i,i+1)$ connectivities was interrupted at position 52, since no sequential contact was observed for Pro^{52}-Arg^{53}. From Arg^{53} to Ser^{65} we found another continuous series of sequential connectivities. The starting point in this stretch was provided by the unique tripeptide Ser^{55}-Ile^{56}-Ile^{57}. Despite the fact that no sequential connectivities were found for the residues 52–53, the two strands (residues 19–52 and 53–65) were 'linked' by the presence of contacts of the type

$d_{\alpha N}$(i,i+3) between Lys[51] and Glu[54], and $d_{\delta N}$(i,i+2) between Pro[52] and Glu[54]. The strand Ser[67]–Cys[69] was assigned with the $d_{\alpha N}$(i,i+1) sequential NOE contacts. The fragment Phe[6]–Thr[12] was assigned starting from a spin system which was unequivocally identified as Val[9]. The pattern of sequential connectivities was interrupted at Thr[12]. The strand Leu[13]–Thr[17] was assigned starting from the NOE connectivities of a dipeptide AMM'XX'-AMX identified as Met[15]-Asp[16]. The remaining isoleucine spin system was assigned by exclusion to Ile[2]. The unassigned AMX spin systems belonged to Cys[3] and Asn[70]; they were first discriminated from the values of the ^{13}C and ^{1}H chemical shifts and then from the sequential contacts $d_{\alpha N}$(i,i+1) between Ile[2] and Cys[3], thus confirming the assignment. The residues Pro[30], Pro[49] and Pro[52] were assigned from the NOE contacts with the following and preceding residues. Pro[18] was recognised by the $d_{\alpha\beta}$(i,i+3) contact with Tyr[21]. The remaining proline and serine spin systems were assigned to Pro[4] and Ser[5]. They were the only residues whose identifications do not rely on the observation of sequential NOEs.

Identification of secondary structure

A complete summary of the NMR parameters used to identify the secondary structure of h-UG protein is given in Fig. 6. The pattern of NOE connectivities identifies the nature of the polypeptide conformation (Wüthrich, 1986). Strong d_{NN}(i,i+1) as well as $d_{\alpha N}$(i,i+3) and $d_{\alpha\beta}$(i,i+3) con-

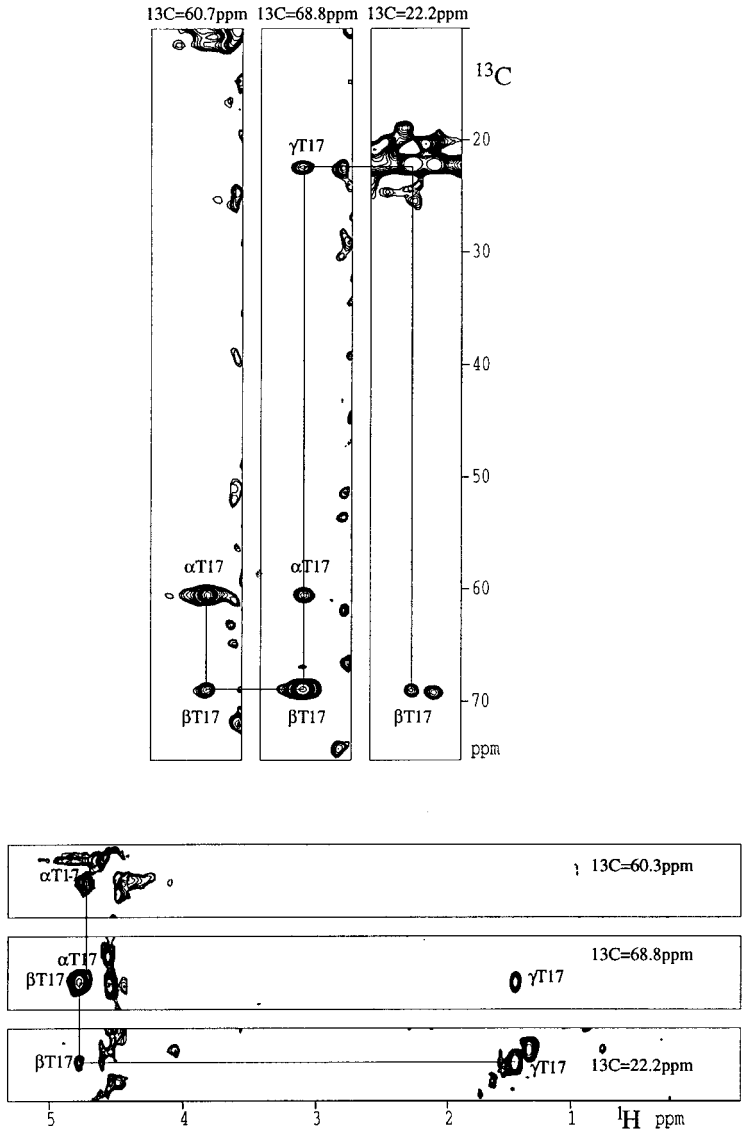

Fig. 5. Strip plot for the complete ^{13}C and ^{1}H aliphatic assignment of Thr[17] with the H(C)CH- and (H)CCH-COSY experiments. In the first experiment the chemical shift of the aliphatic protons, where the magnetisation resides in the beginning, was monitored in t_1; in the second experiment the chemical shift of the carbons to which the magnetisation is transferred after the first INEPT step was monitored in t_1. Extensive folding was used in both experiments, along the t_2 dimension in the first experiment and along the t_1 dimension in the second. The strips are taken from planes at different ^{13}C chemical shifts (indicated at the top).

Fig. 6. Schematic representation of the NOE contacts that are relevant for the secondary structure identification. The intensities of the sequential NOEs are proportional to the height of the box, while no proportionality has been reported for nonsequential contacts; empty boxes represent NOEs for which the symmetrical signal was observed but was ambiguous due to overlap. Filled circles indicate slowly exchanging amide protons. The chemical shift differences between the random coil values and the h-UG protein are reported for H^{α} and C^{α}. At the bottom the secondary structure elements identified are shown as helices α1–α4.

nectivities are indicative of α-helical conformation. In this study, the NOEs involving the amide protons were evaluated from the 100 ms ^{15}N-edited 3D NOESY spectra, while the $d_{\alpha\beta}(i,i+3)$ connectivities were evaluated from the 100 and 200 ms 2D NOESY experiments.

The hydrogen exchange rates were obtained as described in the Materials and Methods section. Amide protons with a hydrogen exchange rate k_{HX} smaller than 0.005 s^{-1} can be detected in the first spectrum of the series and are referred to as 'slowly exchanging' amide protons. A total of 20 slow exchanging amide protons were detected out of 64 possible candidates. The slow exchange regime could be due either to an amide proton buried inside the structure and thus not easily reachable by the solvent, and/or to its involvement in a hydrogen bond, which would slow down its mobility.

The correlation between chemical shift and secondary structure has long been recognised (Pastore and Saudek 1990; Spera and Bax, 1991; Wishart et al., 1991,1992; Wishart and Sykes, 1994). The chemical shift differences (between the random coil values and the h-UG protein) for H^{α} and C^{α} are shown in Fig. 6, and essentially agree with the NOE data and exchange rates, which point to the existence of four helical regions.

α-Helical structures

Helix α1 (residues 7–14) is the least well characterised. The NOE connectivities $d_{NN}(i,i+1)$ and $d_{\beta N}(i,i+1)$, together with the H^{α} and C^{α} chemical shift values, indicate that segment 7–14 is helical, even if no $d_{\alpha\text{-}x}(i,i+3)$ could be unequivocally detected. The presence of $d_{\alpha N}(i,i+1)$ contacts suggests that this helix may be distorted. Furthermore,

TABLE 1
DEGREE OF HELICITY OF SEVERAL PROTEINS OF THE UG FAMILY

Helix	h-UG		Rabbit UG		Rat UG
	*P*222	Solution	$C222_1$	$P2_1$	$P6_522$
α1	4–14	7–14	4–14	5–14	4–14
α2	18–27	18–28	18–27	19–25	18–26
α3	32–46	32–47	32–47	32–45	32–47
α4	50–66	50–63	50–65	50–63	50–64
Helical content	75%[a]	68%[a]	75%[a]	64%[a]	73%[a] (66%)[b]

[a] Percentages considering the 70-residue molecule.
[b] Percentage considering the effective length of the protein (75 residues).

the $d_{\alpha N}(i,i+2)$ contact found seems to indicate that the terminal part of the helix tends to assume a 3_{10} form. The high exchange rates of the amide protons suggest that this helix should be relatively exposed to the solvent.

Helix α2 (residues 18–28) is characterised by a continuous pattern of $d_{NN}(i,i+1)$ connectivities and by $d_{\alpha N}(i,i+3)$ and $d_{\alpha\beta}(i,i+3)$ contacts which, together with the H^{α} and C^{α} chemical shift values, indicates that this segment is an α-helix. Nevertheless, the incomplete pattern of $d_{\beta N}(i,i+1)$ NOEs and some amide protons with fast exchange rates, together with the presence of $d_{\alpha N}(i,i+2)$ NOEs, points to a partially distorted helix with a mixture of α-helix and 3_{10}-helix character towards the end of the helix.

Helix α3 (residues 32–47) is the longest helical segment. It is characterised by a continuous stretch of sequential $d_{NN}(i,i+1)$ and $d_{\beta N}(i,i+1)$ connectivities and by the presence of almost all the possible $d_{\alpha\beta}(i,i+3)$ contacts. The pattern is entirely consistent with the chemical shift differences of H^{α} and C^{α}. Moreover, most of the slowly exchanging amide protons are located in this helix. Nevertheless, together with the $d_{\alpha N}(i,i+3)$ contacts, we observe some $d_{\alpha N}(i,i+2)$ connectivities towards the end of the helix, which are indicative of 3_{10}-helix character.

Helix α4 (residues 50–63) is well characterised by the continuous pattern of $d_{NN}(i,i+1)$ and $d_{\beta N}(i,i+1)$ connectivities and most of the $d_{\alpha N}(i,i+3)$ and $d_{\alpha\beta}(i,i+3)$ are present. The chemical shift differences of H^{α} and C^{α} are in agreement with the helical conformation. Few amide protons in this helix present slow exchanging rates. The presence of one $d_{\alpha N}(i,i+2)$ contact at the beginning of this stretch might indicate that the helix starts with 3_{10} character and then turns into an α-helix.

The strands that go from Glu^{1} to Phe^{6} and from Ala^{64} to Asn^{70} and which are involved in the two disulphide bridges do not show any particular secondary structure. The values of the H^{α} and C^{α} chemical shifts of Met^{15} indicate that this residue is not part of a helix, while the slow exchange rate of its amide proton indicates that it could be involved in a hydrogen bond. We can hypothesise the presence of a type I turn from Thr^{12} to Met^{15}, which is consistent with the presence of strong $d_{\alpha\beta}(i,i+4)$ contacts between Thr^{12} and Asp^{16}.

Discussion and Conclusions

Recombinant h-UG in solution appears to be a very stable helical protein. Although it was virtually impossible to reach complete thermal denaturation, it is clear that the actual T_m must be well above 70 °C. Moreover, at pH 6.2 a complete recovery of the native folding was obtained by lowering the temperature from 60 to 20 °C, as could be judged by the perfectly overlapping CD curves (data not shown). The unusually high stability to thermal denaturation is very likely enhanced by the presence of the two disulphide bonds.

In Table 1 a comparison between the location of the helices found by NMR spectroscopy in the present work and those obtained from an X-ray diffraction study of h-UG (Umland et al., 1994) is shown; for completeness the crystallographic results for rabbit UG (Morize et al., 1987; Bally and Delettre', 1989) and rat UG protein (Umland et al., 1992) are reported as well. With the exception of the starting residues of α1 and the ending residues of α4, the results are in general agreement. However, it is clear that as far as the beginning and the end of the helices are concerned there is no complete agreement even for the two different space group forms of the same crystallised protein, namely rabbit UG. This result is not surprising if one considers the X-ray crystallographic temperature factor (B-factor). This parameter relates to the amplitude of vibration of the backbone atoms in a given residue, and is therefore an indicator of dynamical processes that were blocked during crystal packing. Only in the case of the two rabbit UG structures (Morize et al., 1987; Bally and Delettre', 1989) the authors explicitly present these data, but they are very informative since they give the values for each amino acid. If we take into account residues 7–14 for helix α1, the average B-factor for the structure described by Morize et al. (1987) is 7.8 $Å^2$, while for residues 4–6 it is 11.9 $Å^2$; the average B-factor for helix α4 (residues 50–63) is 8.4 $Å^2$, and for residues 64–66 it is 14.4 $Å^2$. In the other case (Bally and Delettre', 1989) we have average B-factors of 7.5 and 11.8 $Å^2$, respectively, for helix α1 and residues 4–6; and of 8.8 and 14.4 $Å^2$, respectively, for helix α4 and residues 64–66. The values of residues 4–6 and 64–66 are similar to those of the unstructured residues in both X-ray crystal structures mentioned. In this respect, Bally and Delettre' (1989) themselves state that these values are comparable to those of residues 29–34 which are outside the dimer and exposed into the solvent region.

It should be stressed that the accuracy of helix boundaries derived from the qualitative interpretation of NMR data is rather poor and an uncertainty of ±1 residue should be allowed (Clore and Gronenborn, 1989). Taking into account all these facts, we conclude that the difference between our data and the crystallographic data for helices α1 and α4 could reflect some dynamics taking place at these residues, which is prevented in the crystal structures by the crystal packing forces but is revealed by their corresponding B-factors. In solution helices α1 and α4 should, respectively, begin and end with a difference of about three residues each compared to the crystallised form, while no substantial difference is observed for helices α2 and α3. It is interesting to note that for the first and last six residues of h-UG, not only few NOE contacts were available but also the scalar connectivities were weak. These two stretches of residues precede and follow the cysteine bridges, which suggests that a disulphide flip of conformation introduces line broadening

caused by chemical exchange, as already reported for BPTI (Otting et al., 1993) and for the amino-terminal fragment of the urokinase-type plasminogen activator (ATF-u-PA) (Hansen et al., 1994). The fact that the residues involved are not structured certainly favours such behaviour, and the consequent line broadening of the signals in our case could well explain the weak dipolar and scalar correlations of the starting and ending six residues.

The differences in helix length and the higher degree of freedom that the initial and terminal residues experience in solution could have some functional relevance. Although no in vivo evidence has ever been obtained, it has been postulated that the internal hydrophobic cavity evidenced in the X-ray structures of the UG family could be an interaction site with some target molecule still to be identified. In fact, several ligands have been identified in vitro, but no conclusive evidence has been shown to date about which could be the natural ligand. Peter et al. (1992) have widely investigated the binding properties of rabbit UG with progesterone using also UG mutants at both the cysteine positions, and in order to account for the binding evidence with the X-ray crystal structures, even in the reduced form of UG, they had to hypothesise that a certain degree of flexibility has to involve helices α1 and α4 in order to allow access to and from the cavity of progesterone. Our results seem to support their hypothesis.

A different possibility for the access of ligands to the cavity was proposed by Umland et al. (1994). They postulated the existence of a redox mechanism that regulates the access to the hydrophobic cavity by the target molecule and enables it to serve as a carrier and protector protein for molecules and phospholipids. Although this possibility cannot be ruled out in principle, it should be pointed out that disulphide bonds are generally stable in the extracellular environment. In fact, both recombinant rabbit UG and h-UG form their disulphide bonds in the cytoplasm of *E. coli* (Miele et al., 1990; Mantile et al., 1993) under relatively reduced conditions. Such a redox mechanism would most likely require an additional UG-binding protein to enzymatically catalyse the reduction of disulphide bonds in the extracellular spaces. Moreover, our NMR data suggest that while access to the hydrophobic cavity by substances may be possible as predicted by Umland et al. (1994), it does not necessarily have to depend on a redox mechanism. A channel formed by the amino and carboxy terminals of the two antiparallel monomers may allow access to and from the cavity. If residues 1–6 and 64–70 are allowed to fluctuate, their steric obstacle to access the cavity could be overcome by a ligand even under oxidised conditions. This, indeed, would account for the binding of progesterone (Beato et al., 1977), retinoic acid and retinol (Lopez de Haro et al., 1994) to rabbit UG, and of PCB to rat UG (Gillner et al., 1988). The binding, although diminished, is not suppressed under oxidised conditions. For the rabbit UG ligands an affinity that is about one order of magnitude less than under reduced conditions has been estimated, while for the rat UG ligand it has been shown that the specific binding decreases by a factor of three under oxidised conditions. The fact that binding takes place also under oxidised conditions demonstrates that the ligands can access the cavity in the presence of disulphide bonds, although with diminished affinity. It is obvious that under reduced conditions access to the cavity is more facilitated.

From the detailed observation of the X-ray structures of the previously mentioned structurally related proteins, it was noticed that all the helices are far from ideal α-helices, although only in the case of rabbit UG crystallised in the $P2_1$ form the authors explicitly declare that the helices are highly distorted, with hydrogen bonds longer than the standard in α-helices and often bifurcated (Bally and Delettre', 1989). These authors notice that all the carbonyl groups tend to tilt outward, away from the helix axis. As a result, the helices are a mix of α- and 3_{10}-helices, which is in complete agreement with our findings for h-UG. Moreover, the authors noted that there is a noncrystallographic pseudobinary axis relating the monomers in the dimer, but that rather significant symmetry distortions are noticeable for residues 24–31 (end of helix α2 and starting of the loop) and the first residues of the N-terminus and the last residues of the C-terminus. Again, this observation is in agreement with our findings, even if in solution a more complicated dynamic situation is present.

In summary, we have presented experimental data obtained on human recombinant UG protein in solution under oxidised conditions. This protein presents the same type of folding as rabbit UG and rat Clara cell 17 kDa protein. The structural features in solution are very similar to those of UG-like proteins from different species, even for the deviations from regularity of the secondary structure elements. A difference from the structural point of view has been found in the length of the beginning and ending helices. This difference could be due to the action of the crystal packing forces that can stabilise a few residues in the helical conformation compared to the solution state.

Acknowledgements

The work by G.M. in the preparation of the samples was equally important for the development of this project as was the work by the spectroscopists. T.C. acknowledges the IRBM for providing support and hospitality for the development of this project, and the MURST (Ministero per l'Universita' e la Ricerca Scientifica e Tecnologica) for a grant. The authors acknowledge Dr. Daniel O. Cicero for a critical reading of the manuscript and useful suggestions.

Note added in proof

While this manuscript was under revision, a related article by T. Hard et al. [(1995) *Nat. Struct. Biol.*, **2**, 983–989] was published. These authors present the solution structure of the rat UG complex with PCB under reduced conditions. They observe the same splitting of the peaks at acidic pH, and conclude that a degree of slight asymmetry exists in solution among the monomers. They also found that helices α1 and α4 are shorter by three and two residues, respectively, compared with the X-ray structure.

References

Anglister, J., Grzesiek, S., Ren, H., Klee, C.B. and Bax, A. (1993) *J. Biomol. NMR*, **3**, 121–127.

Archer, S.J., Baldisseri, D.M. and Torchia, D.A. (1992) *J. Magn. Reson.*, **97**, 602–606.

Aue, W.P., Bartholdi, E. and Ernst, R.R. (1976) *J. Chem. Phys.*, **64**, 2229–2246.

Bally, R. and Delettre', J. (1989) *J. Mol. Biol.*, **206**, 153–170.

Bax, A., Griffey, R.H. and Hawkins, B.L. (1983) *J. Magn. Reson.*, **55**, 301–315.

Bax, A. and Davis, D.G. (1985) *J. Magn. Reson.*, **65**, 355–360.

Bax, A., Ikura, M., Kay, L.E., Torchia, D.A. and Tschudin, R. (1990a) *J. Magn. Reson.*, **86**, 304–318.

Bax, A., Clore, G.M., Driscoll, P.C., Gronenborn, A.M., Ikura, M. and Kay, L.E. (1990b) *J. Magn. Reson.*, **87**, 620–627.

Bax, A., Ikura, M., Kay, L.E. and Guang, Z. (1991) *J. Magn. Reson.*, **91**, 174–178.

Beato, M. (1977) In *Development in Mammals*, 2nd ed. (Ed., Johnson, M.H.), Elsevier, Amsterdam, The Netherlands, pp. 173–198.

Beato, M., Arnemann, J. and Voss, H.J. (1977) *J. Steroid Biochem.*, **8**, 725–730.

Beier, H. (1968) *Biochim. Biophys. Acta*, **160**, 289–291.

Bodenhausen, G. and Ruben, D.J. (1980) *Chem. Phys. Lett.*, **69**, 185–189.

Braunschweiler, L. and Ernst, R.R. (1983) *J. Magn. Reson.*, **53**, 521–528.

Cabre, F., Moreno, J.J., Carabaza, A., Ortega, E., Mouleon, D. and Carganico, G. (1992) *Biochem. Pharmacol.*, **44**, 519–525.

Camussi, G., Tetta, C., Bussolino, F. and Baglioni, C. (1990a) *J. Exp. Med.*, **171**, 913–917.

Camussi, G., Tetta, C. and Baglioni, C. (1990b) *Adv. Exp. Med. Biol.*, **279**, 161–172.

Chan, C.C., Ni, M., Miele, L., Cordella-Miele, E., Ferrick, M., Mukherjee, A.B. and Nussenblatt, R.R. (1991) *Arch. Ophthalmol.*, **109**, 278–281.

Clore, G.M. and Gronenborn, A. (1989) *Crit. Rev. Biochem. Mol. Biol.*, **24**, 479–564.

Cowan, B.D., North, D.H., Whithworth, N.S., Fujita, R., Shumaker, E.K. and Mukherjee, A.B. (1986) *Fertil. Steril.*, **45**, 820–823.

Dhanireddy, R., Kikukawa, T. and Mukherjee, A.B. (1988) *Biochem. Biophys. Res. Commun.*, **152**, 1447–1454.

Diaz Gonzalez, K. and Nieto, A. (1995) *FEBS Lett.*, **361**, 255–258.

Di Rosa, M. and Ialenti, A. (1990) In *Cytokines and Lipocortin in Inflammation and Differentiation* (Eds., Melli, M. and Parente, L.), Plenum, New York, NY, U.S.A, pp. 99.81–99.90.

Facchiano, A., Cordella-Miele, E., Miele, L. and Mukherjee, A.B. (1991) *Life Sci.*, **48**, 453–464.

Gillner, M., Lund, J., Cambillau, C., Alexandersson, M., Hurtig, U., Bergman, A., Klasson-Wehler, E. and Gustafson, J.A. (1988) *J. Steroid Biochem.*, **31**, 27–33.

Griesinger, C., Sørensen, O.W. and Ernst, R.R. (1989) *J. Magn. Reson.*, **84**, 14–63.

Gronenborn, A.M., Bax, A., Wingfield, P.T. and Clore, G.M. (1989) *FEBS Lett.*, **243**, 93–98.

Grzesiek, S. and Bax, A. (1993) *J. Biomol. NMR*, **3**, 185–204.

Guy, J., Dhanireddy, R. and Mukherjee, A.B. (1992) *Biochem. Biophys. Res. Commun.*, **189**, 662–669.

Hansen, A.P., Petros, A.M., Meadows, R.P. and Fesik, S.W. (1994) *Biochemistry*, **33**, 15418–15424.

Ialenti, A., Doyle, P.M., Hardy, G.N., Simpkin, D.S.E. and Di Rosa, M. (1990) *Agents Actions*, **1–2**, 48–49.

Ikura, M., Bax, A., Clore, G.M. and Gronenborn, A.M. (1990) *J. Am. Chem. Soc.*, **112**, 9020–9022.

Ikura, M., Kay, L.E. and Bax, A. (1991) *J. Biomol. NMR*, **1**, 299–304.

Jeener, J., Meier, B.H., Bachmann, P. and Ernst, R.R. (1979) *J. Chem. Phys.*, **71**, 4546–4553.

Kay, L.E., Torchia, D.A. and Bax, A. (1989a) *Biochemistry*, **28**, 8972–8979.

Kay, L.E., Marion, D. and Bax, A. (1989b) *J. Magn. Reson.*, **84**, 72–84.

Kikukawa, T., Coward, B.D., Tejada, R.I. and Mukherjee, A.B. (1988) *J. Clin. Endocrinol. Metab.*, **67**, 315–321.

Krishnan, R.S. and Daniel Jr., J.C. (1967) *Science*, **158**, 490–492.

Kundu, J., Mantile, G., Miele, L., Cordella-Miele, E. and Mukherjee, A.B. (1996) *Proc. Natl. Acad. Sci. USA*, **93**, 2915–2919.

Levin, S.W., Butler, J.D., Schumaker, U.K., Wightman, P.D. and Mukherjee, A.B. (1986) *Life Sci.*, **38**, 1813–1819.

Lloret, S.J.J. and Moreno, J.J. (1992) *Biochem. Pharmacol.*, **44**, 1437–1441.

Lopez de Haro, M.S., Perez, M.M., Garcia, C. and Nieto, A. (1994) *FEBS Lett.*, **349**, 249–251.

Mantile, G., Miele, L., Cordella-Miele, E., Singh, G., Katyal, S.L. and Mukherjee, A.B. (1993) *J. Biol. Chem.*, **268**, 20343–20351.

Manyak, M.J., Kikukawa, T. and Mukherjee, A.B. (1988) *J. Urol.*, **140**, 176–182.

Marion, D., Ikura, M., Tschudin, R. and Bax, A. (1989a) *J. Magn. Reson.*, **85**, 393–399.

Marion, D., Driscoll, P.C., Kay, L.E., Wingfield, P.T., Bax, A., Gronenborn, A.M. and Clore, G.M. (1989b) *Biochemistry*, **28**, 6150–6156.

Messerle, B.A., Wider, G.A., Otting, G., Weber, C. and Wüthrich, K. (1989) *J. Magn. Reson.*, **85**, 608–613.

Miele, L., Cordella-Miele, E. and Mukherjee, A.B. (1987) *Endocr. Rev.*, **8**, 474–490.

Miele, L., Cordella-Miele, E., Facchiano, A. and Mukherjee, A.B. (1988) *Nature*, **335**, 726–730.

Miele, L., Cordella-Miele, E. and Mukherjee, A.B. (1990) *J. Biol. Chem.*, **265**, 6427–6435.

Miele, L., Cordella-Miele, E., Mantile, G., Peri, A. and Mukherjee, A.B. (1994) *J. Endocrinol. Invest.*, **17**, 679–692.

Morize, I., Surcouf, E., Vaney, M.C., Epelboin, Y., Buehner, M., Fridlansky, F., Milgrom, E. and Mornon, J.P. (1987) *J. Mol. Biol.*, **194**, 725–739.

Mukherjee, A.B., Cordella-Miele, E., Kikukawa, T. and Miele, L. (1988) *Adv. Exp. Med. Biol.*, **231**, 135–145.

Müller, L. (1979) *J. Am. Chem. Soc.*, **101**, 4481–4484.

Nordlund-Moller, L., Anderson, O., Ahlgren, R., Skilling, J., Gillner, M., Gustaffson, J.A. and Lund, J. (1990) *J. Biol. Chem.*, **265**, 12690–12693.

Oschkinat, H., Griesinger, C., Kraulis, P.J., Sørensen, O.W., Ernst, R.R., Gronenborn, A.M. and Clore, G.M. (1988) *Nature*, **332**, 374–377.

Otting, G., Liepinsh, E. and Wüthrich, K. (1993) *Biochemistry*, **32**, 3571–3582.

Pastore, A. and Saudek, V. (1990) *J. Magn. Reson.*, **90**, 165–176.

Perretti, G., Becherucci, C., Mugridge, G., Soliteo, E., Silvestri, S. and Parente, L.A. (1991) *Br. J. Pharmacol.*, **103**, 1327–1332.

Peter, W., Dunkel, R., Stouten, P.F.W., Vriend, G., Beato, M. and Suske, G. (1992) *Protein Eng.*, **5**, 351–359.

Ray, M.K., Magdaleno, S., O'Malley, B.W. and De Mayo, F.J. (1993) *Biochem. Biophys. Res. Commun.*, **197**, 163–171.

Singh, G., Sing, J., Katyal, S.L., Brown, W.E., Kramps, J.A., Paradis, I.L., Dauber, J.H., MacPherson, T.A. and Squeglia, N. (1988a) *J. Histochem. Cytochem.*, **36**, 73–80.

Singh, G., Katyal, S.L., Brown, W.E., Phillips, S., Kennedy, A.L., Anthony, J. and Squeglia, N. (1988b) *Biochem. Biophys. Acta*, **950**, 329–337.

Singh, G., Katyal, S.L., Brown, W.E. and Kennedy, A.E. (1990) *Biochem. Biophys. Acta*, **1039**, 348–355.

Singh, G., Katyal, S.L., Brown, W.E. and Kennedy, A.E. (1993) *Exp. Lung Res.*, **19**, 67–75.

Sklenář, V., Piotto, M., Leppik, R. and Saudek, V. (1993) *J. Magn. Reson.*, **A102**, 241–245.

Spera, S. and Bax, A. (1991) *J. Am. Chem. Soc.*, **113**, 5490–5492.

Tetta, C., Camussi, G., Bussolino, F., Herrick-Davis, K. and Baglioni, C. (1991) *J. Pharmacol. Exp. Ther.*, **257**, 616–620.

Umland, T.C., Swaminathan, S., Furey, W., Singh, G., Pletcher, J. and Sax, M. (1992) *J. Mol. Biol.*, **224**, 441–448.

Umland, T.C., Swaminathan, S., Singh, G., Warty, V., Furey, W., Pletcher, J. and Sax, M. (1994) *Nat. Struct. Biol.*, **1**, 538–545.

Wishart, D.S., Sykes, B.D. and Richards, F.M. (1991) *J. Mol. Biol.*, **222**, 311–333.

Wishart, D.S., Sykes, B.D. and Richards, F.M. (1992) *Biochemistry*, **31**, 1647–1651.

Wishart, D.S. and Sykes, B.D. (1994) *J. Biomol. NMR*, **4**, 171–180.

Wishart, D.S., Bigam, C.G., Yao, J., Abilgaard, F., Dyson, H.J., Oldfield, E., Markley, J.L. and Sykes, B.D. (1995) *J. Biomol. NMR*, **6**, 135–140.

Wüthrich, K. (1986) *NMR of Proteins and Nucleic Acids*, Wiley, New York, NY, U.S.A.

Zuiderweg, E.R.P. and Fesik, S. (1989) *Biochemistry*, **28**, 2387–2391.